Ocean Basin Impact of Ambient Noise on Marine Mammal Detectability, Distribution, and Acoustic Communication

Jennifer L. Miksis-Olds
Applied Research Laboratory
The Pennsylvania State University
PO Box 30
State College, PA 16804
phone: (814) 865-9318 fax: (814) 863-8783 email: jlm91@psu.edu

Award Number: N000141110619

LONG-TERM GOALS

The ultimate goal of this research was to enhance the understanding of global ocean noise and how variability in sound level impacts marine mammal acoustic communication and signal detection. How short term variability and long term changes of ocean basin acoustics impact signal detection was considered by examining 1) the variability in low frequency ocean sound levels and sources, and 2) the relationship of sound variability on signal detection as it relates to marine mammal active acoustic space and acoustic communication. This work increases the spatial range and time scale of prior studies conducted at a local or regional scale. The comparison of acoustic time series from different ocean basins provides a synoptic perspective for observing and monitoring ocean noise on multiple times scales in both hemispheres as economic and climate conditions change. Quantified changes in the acoustic environment were then applied to the investigation of ocean noise issues related to general signal detection tasks, as well as marine mammal acoustic detection and impacts.

OBJECTIVES

The growing concern that ambient ocean sound levels are increasing and could impact signal detection of important acoustic signals being used by animals for communication and by humans for military and mitigation purposes is being addressed. The overall goal of the study was to gain a better understanding of how low frequency sound levels vary over space and time. This knowledge is then related to the range over which marine mammal vocalizations can be detected over different time scales and seasons. Over a decade of passive acoustic time series from the Indian, Atlantic, and Pacific Oceans were used to address the following project objectives:

1. **Determine the major sources (or drivers) of variation in low frequency ambient sound levels on a regional and ocean basin scale.**

   A. What are the regional source contributions to low frequency ambient sound levels?

   B. Is there variation in source characteristics of the major low frequency source components over space and time?

   C. Is low frequency sound level uniformly increasing on a global scale?

2. Investigate the impacts of variation in low frequency ambient sound levels on signal detection range, marine mammal communication, and distribution.

A. How does species specific detection range (acoustic active space) vary on a daily, weekly, monthly, and yearly time scale?

B. Are low frequency vocalization detections related to changes in ambient sound level?

C. Do marine mammals exhibit any changes in calling behavior to compensate for noise?

APPROACH

The originally proposed effort was a comparative study of passive acoustic time series from the Comprehensive Nuclear Test Ban Treaty Organization International Monitoring System (CTBTO IMS) locations in the Indian (H08) and Equatorial Pacific (H11) Oceans over the past decade (Figure 1). An additional site at Ascension Island (H10) in the Atlantic Ocean was added to the time series analyses because it provides an additional southern hemisphere site for comparison. (Figure 1). CTBTO monitoring stations consist of two sets of three omni-directional hydrophones (0.002-125 Hz) on opposite sides of an island. The hydrophones are located in the SOFAR channel at a depth of 600 to 1200 m, depending on location. The hydrophones are cabled to land 50-100 km away and connected to shore stations for data transmission. Individual datasets are calibrated to absolute sound pressure levels (SPL) in standard SI units, removing site-specific hydrophone responses. The sites are under the national control of the countries to which the hydrophones are cabled and data is available via AFTAC/US NDC (Air Force Tactical Applications Center/ US National Data Center) for US citizens.

Quantifying the relationship between factors affecting ocean sound variability and corresponding ecosystem response illustrates the effectiveness of passive acoustic monitoring and provides critical information needed for predictive modeling of signal detection probability. Project success is dependent on the appropriate time series analyses and comparisons over time at a single location and across locations. While there is great scientific merit in quantifying the acoustic relationship between physical and biological parameters of the marine ecosystem, the integration of the acoustic datasets with ancillary data sets further enhanced the value of the research by ensuring the appropriate comparisons were made between locations and over time at the same location. Remotely sensed chlorophyll concentration and sea surface temperature (SST) were modeled for the targeted ocean regions to provide insight on the level of primary productivity within each area. Historical vessel data and movements through 2011 were purchased through Lloyd's Marine Intelligence Unit (MIU). The database extends back to 1997, which is appropriate for obtaining shipping data over the same time periods and scales of the acoustic data and other ancillary datasets.

Each step of this research effort has produced significant contributions to the field of ocean science through analyses of sound level trends, variability in signal detection area through acoustic modelling, marine mammal distribution trends, soundscapes, and unit of analysis methodology. The study has culminated in a complex analysis of all environmental factors that could be predictors of marine mammal presence and distribution at the Equatorial Pacific (H11) and Indian Ocean (H08) CTBTO sites. The final year of the research effort focused on identifying the most significant parameters predictive of marine mammal vocal detections.

WORK COMPLETED

The final year's project focus was on 1) comparing long term trends in sound level and source drivers using frequency correlation matrices to identify changes in source characteristics over time, and 2) developing models to identify predictors of marine mammal vocal temporal patterns from multiple environmental and shipping time series. Data from three different CTBTO sites have been downloaded from the AFTAC/US NDC to ARL Penn State. The site locations and current data acquisition are shown in Table 1. Data continues to be downloaded on a monthly basis to keep the database current.

Sources Driving Long-Term Trends

The rate and direction of change in low frequency sound over the past decade in the Indian, South Atlantic, and Equatorial Pacific Oceans resulting from this project has been presented at conferences, included in past ONR Annual Reports, and published (Miksis-Olds & Nichols, accepted with revision; Miksis-Olds et al., 2013) (Figure 2). Based on these observations, it does not appear that low frequency sound levels are increasing in all regions of the world. The answer to the question of "Are ocean sound levels increasing globally?" is highly dependent on the sound level parameter (sound floor, median, or most extreme) of interest (Figure 2). Identifying sources driving the trends was the subject of this year's more detailed analysis.

Annual frequency correlation matrices were constructed to better identify and understand changes in source contributions to the regional soundscapes. To build the correlation matrices from ambient sound recordings, the raw data was first converted into a series of sound spectra using a 10-second FFT, with Hann windowing and 50% window overlap for a three minute long segment each hour within a year. This process resulted in sound spectra, in dB, for each hour in the year of interest, with a 0.1 Hz frequency resolution. The set of spectra can also be seen as a time series of sound level measurements at each frequency. The correlation coefficient was calculated between sound levels at each available pair of frequencies to construct the correlation matrix. The correlation coefficient used in this paper is defined as:

$$r(f_1, f_2) = \frac{\sum_{i=1}^{n}\left(x(f_1)_i - \overline{x(f_1)}\right)\left(x(f_2)_i - \overline{x(f_2)}\right)}{\sqrt{\sum_{i=1}^{n} x(f_1)_i - \overline{x(f_1)})^2 \sum_{i=1}^{n}(x(f_2)_i - \overline{x(f_2)})^2}}, \quad (1)$$

where $x(f_1)$ is the set of ambient sound levels, in dB, at frequency f_1. The calculated correlation coefficients form a diagonally symmetric matrix, where the i-by-j element represents the correlation coefficient between noise levels at f_i and f_j. Since the diagonal elements represent the correlation between sound levels at the same frequency, the diagonal elements must always be exactly unity. The correlation matrix was then conveniently visualized in a color plot with logarithmic axes.

High correlation between the sound levels at two frequencies indicates that the corresponding sound levels tend to increase and decrease at the same times, implying that energy in the two frequency bands is driven by the same source mechanism. Similarly, large frequency regions in which the sound levels are strongly correlated indicate a frequency range which is driven by a particular source. While the strength of a correlation region does not perfectly relate to the absolute intensity of the source, frequently occurring, high intensity sounds typically create a stronger correlation than rarely occurring, low intensity sounds. A notable exception to this tendency would be that if two frequency bands

contained continuously high levels of sound; the correlation between the two bands would be very low, due to the low variance in sound level, though this is exceedingly rare in a medium as dynamic as the ocean.

The correlation regions are used to determine the frequency extent of the different source mechanisms active in a sound field. As an example, the 17-28 Hz squares of high correlation in Figures 3C and 3D denote a frequency region dominated by biologic sounds. To compare two different soundscape time periods, the correlation matrices for the two periods were then subtracted from each other, highlighting frequency regions where the dominant source has changed. The procedure used to create a frequency correlation difference matrix is illustrated in Figure 3.

Predictive Modelling

Data Sources

The response variable in all the generalized linear and additive models (GLM and GAM) was the species specific vocal detection presented as number of hours detected per day. The hourly presence/absence of marine mammal vocalization detections was assessed in collaboration with Sharon Nieukirk (OSU). The acoustic predictor variables were the daily sound level percentile time series for 1%, 50%, and 99% (P1, P50, and P99) of the full spectrum (5-115 Hz). P1 is indicative of the ambient sound floor (i.e. no whales or human activity). P50 is the median, which includes contributions from whales and human activity. P99 represents loudest sounds recorded each day, which were most often seismic airgun pulses or passing ships.

Environmental predictor variables were eight-day SST and [Chl] assessed from the standard NASA satellite imagery Moderate Resolution Imaging Spectroradiometer (MODIS)-Aqua level 3 products at 9 km spatial resolution. This analysis was performed by collaborator Dr. Colleen Mouw (MTU). Pixels were extracted that were within the signal detection area for each frequency and season for each CTBTO IMS site. Any pixels within a water column less than 50 m deep were eliminated to ensure there were no bottom impacts in the satellite products. The shipping predictor variable was a quarterly time series obtained from Lloyd's List Intelligence (London, UK).

Signal Detection Area

Signal detection areas around CTBTO IMS monitoring stations at Diego Garcia (H08: Indian Ocean), Ascension Island (H10: Atlantic Ocean), and Wake Island (H11: Equatorial Pacific Ocean) were estimated using the passive sonar equation (Ainslie, 2010; Urick, 1967) in collaboration with Dr. Kevin Heaney (OASIS). A constant source level of 180 dB re 1 μPa was used to be reflective of the range of estimated blue and fin whale vocalization source levels (Širović, 2007; Clark et al., 2009; Samaran et al., 2010; Castellote et al., 2011). For this work the directivity index and processing gain were set to zero, which is likely an underestimate of the performance for marine mammals communicating. The detection threshold was set so that a false alarm rate of 5% was achieved – meaning that for the local ambient noise time window, only 5% of the noise levels exceeded this level. The noise level parameter for the passive sonar equation was calculated from acoustic recordings from a single north hydrophone at each CTBTO IMS monitoring location. Mean spectral levels were calculated using a Hann windowed 15,000 point Discrete Fourier Transform with no overlap to produce sequential 1-min power spectrum estimates over the duration of the dataset. The transmission loss for each season at each location was modelled along 360 bearings at 1^{o} resolution using the OASIS Peregrine parabolic equation model for a receiver in the deep sound channel and a source position extending over the upper 300 m of the water column to be consistent with the hypothesized

depth of vocalizing baleen whales (Oleson et al., 2007; A. K. Stimpert, pers. comm., 7 January 2015). Seasons were considered as follows: spring (Mar. – May), summer (Jun. – Aug.) fall (Sep. – Nov.), winter (Dec. – Feb.). Detection area was computed by estimating the maximum range along each bearing where the signal excess fell below zero. Straight lines were used to connect the range points along the 360 bearings to form a polygon, and the area within the polygon was calculated from the bearing range lengths (Figure 4). The signal detection area varied by season and signal frequency (Miksis-Olds et al, in press).

Temporal Matching

The temporal resolution of all the data sources differed. The acoustical data (sound level and vocal detections) were daily, shipping was quarterly, and satellite products were 8-day. All data were merged to match the 8-day resolution of the satellite imagery. All daily sound level observations for a given 8-day period were averaged for that period. The daily whale occurrence data was summed for each 8-day period. The quarterly ship movements were divided equally between each 8-day period of a quarter.

Statistical Modeling – Colleen Mouw (MTU)

Generalized linear and additive models (GLM and GAM) were used to investigate the relationship between the number of hours per day each whale species was detected vocally (response variable) and the predictor variables. The predictor variables of the initial models included: total ship movements, SST, [Chl], primary production, P1, P50 and P99 for full spectrum sound levels. Only full spectrum sound levels were considered because blue and fin whales produce vocalizations across the entire spectrum of the 5-115 Hz band available in the CTBTO data. Data were initially checked for outliers by removing data points that were greater/less than three standard deviations away from the mean. Collinearity was evaluated using the *collintest* function in the MATLAB® Econometrics toolbox. Collinearity was initially found between primary production, SST and [Chl], which is not surprising given SST and [Chl] are used in the calculation of primary production, thus primary production was removed from the list of predictor variables (Figure 5). There was also collinearity found between the sound level parameters (P1 and P50) (Figure 5) at both locations. All sound level parameters were maintained in subsequent analyses, however, because the P1 and P50 levels were considered to be representative of different soundscape components. P1 is representative of the acoustic soundfloor associated with characteristics of wind and waves, or geophony (Pyjanowski et al. 2011), whereas the P50 parameter captures elements of the physical (geophony), biological (biophony), and human (anthrophony) components of the soundscape. The P99 parameter is a product of the most extreme sources in the environment mostly related to seismic signals (both natural and man-made) and ship passages.

The distribution of all variables were checked by considering the skewness, calculated as the third central moment of a given variable divided by the cube of its standard deviation. The skewness was lower or nearly equivalent for all variables that had been centered by taking the natural logarithm compared to the raw data. Thus for simplicity, all variables (predictor and response) were centered.

GLM and GAM were fit with a normal distribution and identity link functions. The MATLAB® function *fitglm* in the Statistics Toolbox was used for both GLM and GAM with the *interactions* model used for GAM. Similarly, the *stepwiseglm* MATLAB® function was used to select significant variables. Variables were removed based on a significance criteria of $p<0.05$ until all variables in the model were considered significant. Normal probably and auto-correlation in the model residuals were examined.

RESULTS

Sources Driving Long-Term Trends

The frequency correlation difference matrices found in Figure 6 highlight changes in the dominant sound sources between the beginning and end of the analysis period. Many of the differences identified in the frequency correlation difference matrices are also highlighted in the spectrograms in Figures 3 and 7. The frequency correlation difference matrix in Figure 6 (A) highlights two primary differences in the sound field of H08 Diego Garcia North between 2003 and 2012. First, the region between 5 and 20 Hz shows a substantial change in inter-frequency correlation, produced by the relative absence of manmade seismic sources present in 2012, compared to 2003. Inset (i) of Figure 7 provides a spectrogram example of the manmade seismic signals encountered frequently during 2003. Second, a series of horizontal and vertical lines between 30-40 Hz indicated the presence of some multiple frequency tonal signals, which were detected in 2012, but not in 2003. These tonal signals are consistent with blue whale calls during the austral summer, as circled in Figure 7 (B) (McDonald et al., 2009; Samaran et al., 2010). A typical vocalization detected during that period is seen in inset (ii) of Figure 7.

South of H08 Diego Garcia (Figure 6B), the correlation feature present between 2-7 Hz was produced by an unknown source mechanism which was present in 2012, but not 2003. Typically, sea-surface wave interactions contribute sound up to 4 Hz, above which, seismic sources tend to dominate. This transition usually results in a local minimum sound level around 4 Hz. However, an unidentified sound source introduced a substantial level of sound below 7 Hz for a total of around 100 days. The source is hypothesized to be seismic activity related to the Sumatra earthquake in late 2003. The two periods of time in which this source was active are circled in Figure 7 (D). This same source is not present in recordings made on the northern side of Diego Garcia.

On the South of H10 Ascension Island, the large plus-sign shape centered around 20 Hz in Figure 2 (D) reveals a shift in the dominant source in the 17-28 Hz range. In 2005, broadband sound from natural and manmade seismic sources dominated the 3-17 Hz band, and also contributed substantially to the 17-28 Hz band, where biologic signals are very frequently found. As such, the sound levels in the 17- 28 Hz range correlated moderately well with sound levels in the rest of the frequency range dominated by seismic sources, particularly between 3-17 Hz. The circle connected to inset (i) in Figure 2 (A) marks the strong presence of seismic sounds in 2005, compared to their relatively reduced presence in 2012. Instead, as seen in Figure 2 (B), the intensity of biologic sounds, produced by Antarctic blue whales (inset (ii)) (Stafford et al., 2004; Samaran et al., 2010) and fin whales (inset (iii)) (Nieukirk et al., 2012), was higher in 2012 than in 2005. As a result of the lower level of manmade seismic signals, and a slight increase in the levels of biologic sounds, the 17-28 Hz band is more completely driven by biologic sources in 2012. Consequently, sound levels in that region were less correlated with the surrounding broadband region driven by seismic sources than in 2005. Since sound levels in the 3-17 Hz and 17-28 Hz bands are less correlated with each other in 2012 than in 2005, the frequency correlation difference matrix seen in Figures 2 (E) and 6 (D) show a region of relatively high change in correlation coefficient at the intersection of the 3-17 Hz and 17-28 Hz bands. This effect was not observed North of H10 Ascension Island. Instead, the light blue patches seen above 30 Hz in Figure 6C point to an increase in manmade seismic source activity above 30 Hz in 2012, compared to 2005.

Near H11 Wake Island, the difference matrices for both the north and south receivers, Figures 6E and 6F, show a substantial change in the 20 to 30 Hz range. Compared to the first full year of analysis,

from May 2007 to April 2008, contributions to the sound field from fin whales changed in 2012 to incorporate a higher frequency sweep component to their song. This change in the 20 to 30 Hz sound field is reflected in the circled region of the spectrogram in Figure 7 (F). An example of the higher frequency fin whale sweep dominating the 20 to 30 Hz band at the end of 2012 is shown in inset (iii) of Figure 7 (F). Though the spectrograms in Figure 7 (E) and (F) only show the south side of Wake Island, a very similar change was observed on the north side of the island.

Predictive Modelling

Three different generalized models were assessed in determining the most appropriate model for predicting marine mammal temporal patterns around Wake Island in the Pacific and Diego Garcia in the Indian Oceans: 1) response variable not centered, zeros (absence) included, 2) response variable centered, zeros removed, and 3) response variable centered, zeroes included. Model 1 was excluded because the zeros indicating whale absence were valid and informative data. Model 3 was selected as the most appropriate model through examination of residual autocorrelation and residual normal probability plots.

At Wake Island in the Pacific, four species were detected with regularity: Bryde's, blue, fin, and minke whale. Overall p values of the GLM and GAM models for a step-wise fit were used to select the best model for each species. The GAM was the best fit for identifying predictor variables for Bryde's, blue, and minke whales, while the GLM was a best fit for fin whales. Significant predictors are summarized in Table 2, and impact direction plots are found in Figure 8. The significant single predictors of Bryde's vocal presence were P99 sound levels, total ship movements, and [Chl]. Bryde's vocal detection decreased with an increase in each predictor variable. SST was the strongest single predictor from the variables considered as indicated by p-value, and the interaction between [Chl] and SST was the strongest overall predictor. The significant single predictors of blue whale vocal presence were P1 and P50 sound levels, total ship movements, and [Chl]. Blue whale vocal detection increased with increases in P1 sound level and [Chl], which was opposite of the Bryde's whale, and decreased with increasing values of P50 and total ship movements. Total shipping movements was the strongest single predictor from the variables considered as indicated by p-value, and the interaction between P50 and total shipping was the strongest overall predictor. Significant single predictors of fin whale vocal detections were P1 sound level, [Chl], and SST with the P1 sound level being the strongest single and overall predictor. Fin whale detections increased with increasing P1 sound levels and [Chl]. Fin whale detections decreased with increasing SST. Significant predictors of minke whale vocal detection were P1 and P50 sound levels and [Chl] with P1 sound level being the strongest single and overall predictor. Minke whale vocal detections increased with increasing P1 and [Chl] values and decreased with increasing P50 sound levels.

In the Indian Ocean at Diego Garcia, blue, fin, and minke whales were detected vocally over the decade time period from 2002-2012. Five different groups of blue whale vocalizations were identified (Antarctic, Madagascar, Sri Lankan, U1, and U2) and were analysed separately. Overall p values indicated that the stepwise GAM was the best fit for all groups except the minke whales, where the stepwise GLM was the best fit. Table 3 summarizes the significant and strongest predictors for each species and vocalization group. Sound level was the single strongest predictor for Antarctic, Madagascar, Sri Lankan, and U1 blue whale vocalizations. The sound level parameter and direction of impact varied by group. SST was the single strongest predictor for U2 blue whale calls and minke whales. Total shipping was the strongest predictor of fin whale vocal presence.

IMPACT/APPLICATIONS

This study adds to the growing body of literature describing long term trends in ocean sound levels. The initial observation of a 3 dB per decade increase in low frequency sound levels in the NE Pacific was of grave concern and sparked efforts to determine whether this was a global and continuing phenomenon. Low frequency ocean sound trends observed in the South Atlantic Ocean at Ascension Island and Equatorial Pacific at Wake Island do not support a conclusion that ocean sound levels have uniformly increased across the globe over the past decade. Analyses of data from the past decade at Ascension Island and Wake Island showed decreases in the ambient sound floor, as well as decreases in other sound level parameters. The combination of information harvested from both long term time series and frequency correlation matrices provided insight into the likely sources driving the observed trends, and is a useful method for identifying major source shifts contributing to the changing soundscape. Through the use of the frequency correlation matrices, a shift in fin whale song was quickly identified as well as a shift in seismic airgun contributions to the regional soundscape over time. Our ability to fully interpret the information and differences in frequency correlation matrices is still in its infancy, so we have confined our discussion points to the areas indicating the greatest amount of change between a year at the start and end of the data time series. The detailed information available in frequency correlation matrices continue to be explored in on-going work by S. Nichols (ARL Penn State).

Understanding the major environmental components associated with marine mammal presence is vital to developing predicitive capabilities of marine mammal occurrence and distribution to aid in Navy risk assessment and mitigation, espciecally in areas with sparse survey coverage. This work went beyond the local analysis of relationships between whale vocal presence and sound level by including regional environmental parameters related to food availability and large scale oceanographic conditions ([Chl], primary production, SST) from satellite remote sensing. GLM and GAM results revealed that environmental factors were strong predictors of Bryde's whale detections at Wake Island and minke whale detections at Diego Garica, where as sound level predictors were more strongly assocaited with the vocal presence of the remaining species at these sites. The failure to accurately consider the prey field/productiviey and larger oceanographic patterns in studies of marine mammals and noise impacts has been a constant criticism. This work demonstrates the ability to include confounding oceanographic factors into noise impact or response studies, and results from the different species reveal that large scale oceanographic conditions do play a more impartant role in marine mammal distribution and temporal patterns of some species compared to others despite regional sound levels.

TRANSITIONS

This project represents a transition from the acoustic characterization of local areas to the regional characterization of ocean basins. Detailed knowledge of noise statistics and variation will contribute to reducing error and uncertainty associated with signal detection, localization, propagation models, and marine animal density estimates generated from passive acoustic datasets.

RELATED PROJECTS

The propagation modeling included in this study in collaboration with Kevin Heaney (OASIS) is directly related to ONR Ocean Acoustics Award N00014-14-C-0172 to Kevin Heaney titled "Deep Water Acoustics".

The current project is also directly related to and collaborative with ONR Ocean Acoustics Award N00014-11-1-0039 to David Bradley titled "Ambient Noise Analysis from Selected CTBTO Hydroacoustic Sites". Patterns and trends of ocean sound observed in this study will also be directly applicable to the International Quiet Ocean Experiment being developed by the Scientific Committee on Oceanic Research (SCOR) and the Sloan Foundation (www.iqoe-2011.org).

Results and efforts related to this award will directly benefit the follow-on work under ONR Award N000141410397 titled "Large scale density estimation of blue and fin whales." The project is collaborative with Len Thomas and Danielle Harris of CREEM, University of St. Andrews.

REFERENCES

Ainslie, MA (2010). *Principles of Sonar Performance Modelling*. Berlin Heidelberg: Springer-Verlag. Pp 707.

Castellote, M, Clark, CW, Lammers, MO (2011). Fin whale (*Balaenoptera physalus*) population indemnity in the western Mediterranean Sea. Marine Mammal Science 28: 325-344. doi: 10.1111/j.1748-7692.2011.00491.x

Clark, CW, Ellison, WT, Southall, BL, et al. (2009). Acoustic masking in marine ecosystems: intuitions, analysis, and implication. Mar. Ecological Prog. Ser. 395: 201-222.

McDonald, MA, Hildebrand, JA, and Mesnick, S (2009). Worldwide decline in tonal frequencies of blue whale songs. Endangered Species Research 9: 13-21.

Miksis-Olds, JL, Bradley, DL and Niu, XM (2013). Decadal trends in Indian Ocean ambient sound. Journal of the Acoustical Society of America 134: 3464-3475.

Miksis-Olds, JL, Nichols, SM (accepted with revisions). Is low frequency ocean sound increasing globally? Journal of the Acoustical Society of America.

Miksis-Olds, JL, Vernon, JA, Heaney, KD (accepted, in press). The impact of ocean sound dynamics on estimates of signal detection range. Aquatic Mammals (Special ESOMM Edition).

Nieurkirk, SL, Mellinger, DK, Moore, SE, Klinck, K, Dziak, RP, and Goslin, J (2012). Sounds from airguns and fin whales recorded in the mid-Atlantic Ocean, 1999-2009. Journal of the Acoustical Society of America 131: 1102-1112.

Oleson, EM, Calambokidis, J, Burgess, WC, McDonald, MA, LeDuc, CA, Hildebrand, JA (2007). Behavioral context of call production by eastern North Pacific blue whales. Marine Ecology Progress Series 330: 269-284.

Pijanowski, BC, Villaneuva-Rivera, LJ, Dumyahn, SL, Farina, A, Krause, BL, Napoletano, B M,…Pieretti, N (2011). Soundscape ecology: The science of sound in the landscape. BioScience, 61 (3): 203-216. doi: 10.1525/bio.2011.61.3.6

Samaran, F, Adam, O, and Guinet, C (2010). Detection range modelling of blue whale calls in the Southwestern Indian Ocean. Applied Acoustics 71: 1099-1106.

Širović, A, Hildebrand, JA, Wiggins, SM (2007). Blue and fin whale call source levels and propagation range in the Southern Ocean, J. Acoustical Soc. of Am. 122: 1208-1215.

Stafford, KM, Bohnenstiehl, DR, Tolstoy, M, Chapp, E, Mellinger, DK, and Moore, SE (2004). Antarctic-type blue whale calls recorded at low latitudes in the Indian and eastern Pacific Oceans. Deep Research I 51: 1337-1346.

Urick, R. (1967). *Principles of Underwater Sound*. New York: McGraw-Hill.

PUBLICATIONS

Miksis-Olds, JL, Nichols, SM (accepted with revisions). Is low frequency ocean sound increasing globally? Journal of the Acoustical Society of America.

Miksis-Olds, JL, Vernon, JA, Heaney, KD (accepted, in press). The impact of ocean sound dynamics on estimates of signal detection range. Aquatic Mammals (Special ESOMM Edition).

Miksis-Olds, JL (in press). Global trends in ocean noise. In: Effects of Noise on Aquatic Life II. A.N. Popper and A. Hawkins eds., Springer Science + Business Media, LLC., New York.

Miksis-Olds, JL, Nichols, SM (2015). Linking changes in soundscape levels to sources through frequency correlation matrices. Proceedings of the 2015 Underwater Acoustics International Conference and Exhibition, Platanias Crete, Greece, June 21-26, 2015.

Parks, SE, Miksis-Olds, JL and Denes, SL (2014). Assessing marine ecosystem acoustic diversity across ocean basins. Ecological Informatics 21: 81-88.

Hawkins, RS, Miksis-Olds, JL and Smith, CM (2014). Variation in low-frequency estimates of sound levels based on different units of analysis. Journal of the Acoustical Society of America 135: 705-711.

Miksis-Olds, JL, Bradley, DL and Niu, XM (2013). Decadal trends in Indian Ocean ambient sound. Journal of the Acoustical Society of America 134: 3464-3475.

Miksis-Olds JL (2013). What is an underwater soundscape? In: Proceedings of the 2013 Underwater Acoustics International Conference and Exhibition, Corfu, Greece, June 23-38 2013.

Hawkins, RS (2013). Variation in low-frequency underwater ambient sound level estimates based on different temporal units of analysis. MS Thesis, The Pennsylvania State University. State College, PA.

Miksis-Olds JL, Smith CM, Hawkins RS and Bradley DL (2012). Seasonal soundscapes from three ocean basins: what is driving the differences? Conference Proceedings of the 11th European Conference on Underwater Acoustics 34: 1583- 1587. ISBN 978-1-906913-13-7.

Hawkins RS, Miksis-Olds JL, Bradley DL and Smith CM (2012). Periodicity in ambient noise and variation based on different temporal units of analysis. Conference Proceedings of the 11th European Conference on Underwater Acoustics 34: 1417- 1423. ISBN 978-1-906913-13-7. (First author is student of Miksis-Olds)

Nichols SM, Bradley DL, Miksis-Olds JL and Smith CM (2012). Are the world's oceans really that different? Conference Proceedings of the 11th European Conference on Underwater Acoustics 34: 338- 345. ISBN 978-1-906913-13-7.

PRESENTATIONS

Haver, SM, Klinck, H, Miksis-Olds, JL, Nieukirk, SL, Matsumoto, H, Dziak, RP (2015). The not-so silent world: Measuring Arctic, Equatorial, and Antarctic soundscapes in the Atlantic Ocean. Society of Marine Mammalogy Society Meeting. San Francisco, CA. December 13-18.

Miksis-Olds, JL (2015). Keynote: Unraveling soundscapes – Learning to be good ocean listeners. Underwater Acoustics Conference & Exhibition 2015. Crete, Greece. June 21-26.

Miksis-Olds, JL, Nichols, S (2015). Linking changes in soundscape levels to sources through frequency correlation matrices. Underwater Acoustics Conference & Exhibition 2015. Crete, Greece. June 21-26.

Miksis-Olds, JL, Nichols, S (2015). Linking changes in soundscape levels to sources through frequency correlation matrices. OCEANOISE 2015. Vilanova, Spain. May 11-15.

Miksis-Olds, JL, Vernon, JA, and Heaney, K (2014). Global ocean sound behavior and its impact on translating soundscapes into acoustic communication range for signal detection. 5th Intergovernmental conference: The Effects of Sounds in the Ocean on Marine Mammals. Amsterdam, The Netherlands. September 8-12, 2014.

Miksis-Olds, JL, Vernon, JA, and Heaney, K (2014). Applying the dynamic soundscape to estimates of signal detection. 2nd Underwater Acoustics International Conference and Exhibition, Rhodes, Greece, June 22-27, 2014.

Miksis-Olds, JL (2014). Is low frequency sound level uniformly increasing on a global scale? 167th Meeting of the Acoustical Society of America. Providence, RI, May 5-9, 2014.

Ainslie, MA and Miksis-Olds, JL (2013). Periodic changes in deep ocean shipping noise: Possible causes and their implications. Bioacoustics Day, Leiden, Netherlands, September 18, 2013.

Miksis-Olds JL (2013). Global trends in ocean noise. The Effects of Sound on Aquatic Animals, Budapest, Hungary, August 12-16, 2013.

Miksis-Olds JL (2013). What is an underwater soundscape? 2013 Underwater Acoustics International Conference and Exhibition, Corfu, Greece, June 23-38 2013.

HONORS/AWARDS/PRIZES

Office of Naval Research Young Investigator Program (YIP) Award – 2011
Presidential Early Career Award in Science and Engineering (PECASE) - Nominated 2013

Table 1. Data successfully downloaded and available to ARL Penn State.

Site/Location	Start Day	Most Recent Download	# Missing Days	Total Days	Total Years
HA08/Diego Garcia	01/21/2002	07/29/2015	41	4897	13.5
HA10/Ascension Island	11/04/2004	07/29/2015	5	3915	10.8
HA11/Wake Island	04/25/2007	07/29/2015	15	3002	8.2

Table 2. Wake Island (H11) model predictor summary. The statistics reflect GAM values for Bryde's, blue and minke whale. Fin whale values reflect GLM results. Highlighted variables are the single and overall strongest predictors. Impact direction refers to the direction of the response variable as the predictor variable increases.

	Variable	Parameter Estimate	Standard Error	tStat	p-value	Overall F	Overall pValue	Impact Direction
Brydes	**Brydes ~ 1 + P99 + TotalShipping + P1*Chl + Chl*SST**							
	Intercept	8.05E+03	3.48E+03	2.31E+00	2.20E-02	1.19E+01	2.66E-12	
	P1	-1.26E+03	6.79E+02	-1.86E+00	6.50E-02			v
	P99	-4.62E+01	1.80E+01	-2.57E+00	1.10E-02			v
	TotalShipping	-2.78E+00	1.52E+00	-1.82E+00	6.98E-02			v
	Chl	2.24E+03	1.06E+03	2.12E+00	3.58E-02			v
	SST	-6.47E+02	1.92E+02	-3.37E+00	9.29E-04			^
	P1:Chl	-3.45E+02	2.07E+02	-1.67E+00	9.71E-02			
	Chl:SST	-2.07E+02	5.77E+01	-3.58E+00	4.45E-04			
Blue	**U2Blue ~ 1 + P1*Chl + P50*TotalShipping + Chl*SST**							
	Intercept	-2.48E+04	6.80E+03	-3.64E+00	3.65E-04	5.52E+00	3.42E-06	
	P1	1.75E+03	7.01E+02	2.49E+00	1.37E-02			^
	P50	3.48E+03	1.20E+03	2.89E+00	4.31E-03			v
	TotalShipping	1.78E+03	5.84E+02	3.05E+00	2.70E-03			v
	Chl	-2.36E+03	1.13E+03	-2.09E+00	3.78E-02			^
	SST	3.49E+02	1.90E+02	1.84E+00	6.82E-02			v
	P1:Chl	4.47E+02	2.22E+02	2.01E+00	4.58E-02			
	P50:TotalShipp	-3.93E+02	1.29E+02	-3.05E+00	2.70E-03			
	Chl:SST	1.06E+02	5.71E+01	1.85E+00	6.57E-02			
Fin	**Fin ~ 1 + P1*Chl + P1*SST**							
	Intercept	-4.52E+04	1.09E+04	-4.14E+00	5.53E-05	33.8	7.21E-24	
	P1	1.00E+04	2.41E+03	4.15E+00	5.24E-05			^
	Chl	-1.20E+03	6.06E+02	-1.98E+00	4.88E-02			^
	SST	1.22E+04	3.28E+03	3.72E+00	2.74E-04			v
	P1:Chl	2.67E+02	1.34E+02	1.99E+00	4.79E-02			
	P1:SST	-2.70E+03	7.25E+02	-3.73E+00	2.62E-04			
Minke	**Minke ~ 1 + P1 + P50 + Chl**							
	Intercept	-6.82E+02	1.20E+02	-5.68E+00	5.58E-08	2.09E+01	1.40E-11	
	P1	3.34E+02	6.30E+01	5.29E+00	3.61E-07			^
	P50	-1.80E+02	6.90E+01	-2.61E+00	9.82E-03			v
	Chl	4.96E+00	1.77E+00	2.80E+00	5.75E-03			^

Table 3. Diego Garcia (H08) model predictor summary. The statistics reflect GAM values for all species and vocalizations groups except minke whale. Monke whale values reflect GLM results. Highlighted variables are the single and overall strongest predictors. Impact direction refers to the direction of the response variable as the predictor variable increases.

	Variable	Parameter Estimate	Standard Error	tStat	p-value	Overall F	Overall pValue	Impact Direction
Antarctic Blue	**AntarcticBlue ~ 1 + P50 + P1*TotalShipping + P99*TotalShipping + Chl*SST**							
	Intercept	3.59E+03	2.96E+03	1.21E+00	2.26E-01	3.19	0.000985	
	P1	-1.14E+03	6.79E+02	-1.68E+00	9.34E-02			^
	P50	-4.90E+01	1.69E+01	-2.90E+00	3.94E-03			v
	P99	4.51E+02	2.70E+02	1.67E+00	9.58E-02			^
	TotalShipping	-3.53E+02	3.40E+02	-1.04E+00	3.00E-01			^
	Chl	1.93E+02	7.70E+01	2.51E+00	1.26E-02			v
	SST	-1.43E+02	5.28E+01	-2.71E+00	7.03E-03			v
	P1:TotalShipping	1.36E+02	7.89E+01	1.72E+00	8.55E-02			
	P99:TotalShipping	-5.24E+01	3.16E+01	-1.66E+00	9.83E-02			
	Chl:SST	-5.82E+01	2.32E+01	-2.51E+00	1.26E-02			
Madagascar Blue	**MadagascarBlue ~ 1 + P99**							
	Intercept	2.00E+01	1.45E+01	1.38E+00	1.68E-01	3.99	0.0466	
	P99	-6.41E+00	3.21E+00	-2.00E+00	4.66E-02			v
Sri Lankan Blue	**SriLankaBlue ~ 1 + P50 + P1*Chl + P99*Chl + TotalShipping*SST**							
	Intercept	1.72E+03	1.51E+03	1.14E+00	2.56E-01	15	7.05E-21	
	P1	7.69E+02	2.22E+02	3.46E+00	5.90E-04			^
	P50	-6.17E+01	2.58E+01	-2.39E+00	1.75E-02			v
	P99	-2.65E+02	1.09E+02	-2.42E+00	1.60E-02			^
	TotalShipping	-4.59E+02	1.50E+02	-3.06E+00	2.35E-03			v
	Chl	-7.52E+02	4.12E+02	-1.82E+00	6.88E-02			^
	SST	-1.07E+03	3.88E+02	-2.76E+00	6.04E-03			^
	P1:Chl	2.99E+02	9.98E+01	2.99E+00	2.93E-03			
	P99:Chl	-1.20E+02	4.86E+01	-2.48E+00	1.38E-02			
	TotalShipping:SST	1.37E+02	4.53E+01	3.03E+00	2.58E-03			
U1 Blue	**U1Blue ~ 1 + P1 + P50*TotalShipping + P99*Chl + TotalShipping*SST**							
	Intercept	1.46E+04	3.61E+03	4.05E+00	6.30E-05	7.14	1.35E-09	
	P1	-1.65E+02	4.27E+01	-3.88E+00	1.25E-04			v
	P50	-2.27E+03	7.35E+02	-3.08E+00	2.19E-03			^
	P99	-2.83E+02	1.10E+02	-2.58E+00	1.04E-02			v
	TotalShipping	-1.48E+03	4.04E+02	-3.65E+00	2.98E-04			^
	Chl	5.39E+02	2.21E+02	2.44E+00	1.50E-02			v
	SST	-8.20E+02	4.03E+02	-2.04E+00	4.24E-02			v
	P50:TotalShipping	2.68E+02	8.56E+01	3.13E+00	1.87E-03			
	P99:Chl	-1.21E+02	4.89E+01	-2.48E+00	1.37E-02			
	TotalShipping:SST	9.20E+01	4.70E+01	1.96E+00	5.10E-02			
U2 Blue	**U2Blue ~ 1 + P1 + P50 + TotalShipping + Chl + P99*SST**							
	Intercept	-1.56E+04	4.33E+03	-3.60E+00	3.62E-04	7.1	5.42E-08	
	P1	6.59E+01	3.41E+01	1.93E+00	5.41E-02			^
	P50	-5.30E+01	2.24E+01	-2.37E+00	1.84E-02			v
	P99	3.44E+03	9.59E+02	3.58E+00	3.83E-04			v
	TotalShipping	-3.61E+00	1.46E+00	-2.48E+00	1.36E-02			v
	Chl	-2.88E+00	1.28E+00	-2.25E+00	2.49E-02			v
	SST	4.71E+03	1.30E+03	3.61E+00	3.42E-04			^
	P99:SST	-1.04E+03	2.89E+02	-3.60E+00	3.62E-04			
Fin	**Fin ~ 1 + P1*Chl + P50*SST + TotalShipping*Chl + Chl*SST**							
	Intercept	1.92E+04	6.05E+03	3.17E+00	1.65E-03	22.9	3.06E-31	
	P1	4.91E+02	1.89E+02	2.60E+00	9.66E-03			^
	P50	-4.66E+03	1.44E+03	-3.24E+00	1.29E-03			v
	TotalShipping	-3.95E+01	1.04E+01	-3.78E+00	1.81E-04			^
	Chl	-5.10E+02	3.58E+02	-1.42E+00	1.55E-01			v
	SST	-6.24E+03	1.90E+03	-3.30E+00	1.08E-03			^
	P1:Chl	1.85E+02	8.43E+01	2.19E+00	2.92E-02			
	P50:SST	1.39E+03	4.33E+02	3.20E+00	1.47E-03			
	TotalShipping:Chl	-1.60E+01	4.68E+00	-3.41E+00	7.10E-04			
	Chl:SST	-4.67E+01	2.55E+01	-1.83E+00	6.77E-02			
Minke	**Minke ~ 1 + P50*SST**							
	Intercept	2.79E+04	6.22E+03	4.49E+00	9.40E-06	82.5	2.39E-41	
	P50	-6.30E+03	1.42E+03	-4.44E+00	1.17E-05			v
	SST	-8.34E+03	1.87E+03	-4.46E+00	1.08E-05			^
	P50:SST	1.88E+03	4.27E+02	4.41E+00	1.35E-05			

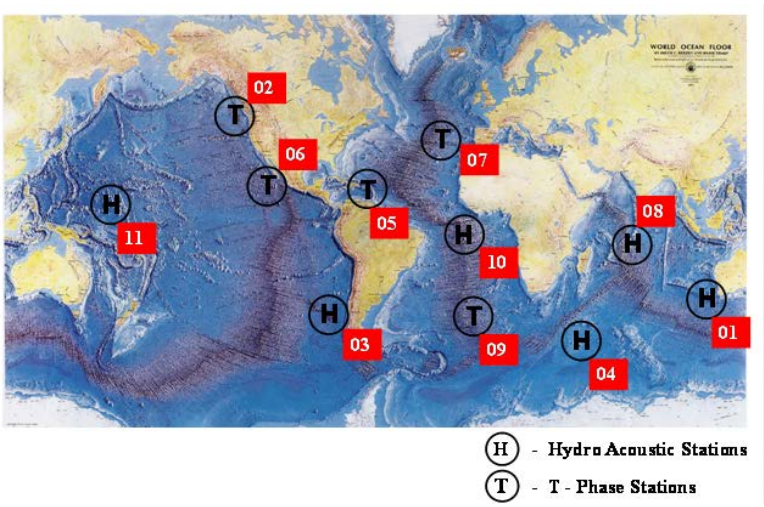

Figure 1. Location of CTBTO Hydroacoustic Sites. H sites denote hydrophone sites, moored in the water column at sound channel depths. T sites denote seismic "T-phase" sensors. This project will use data from H08, H10, and H11.

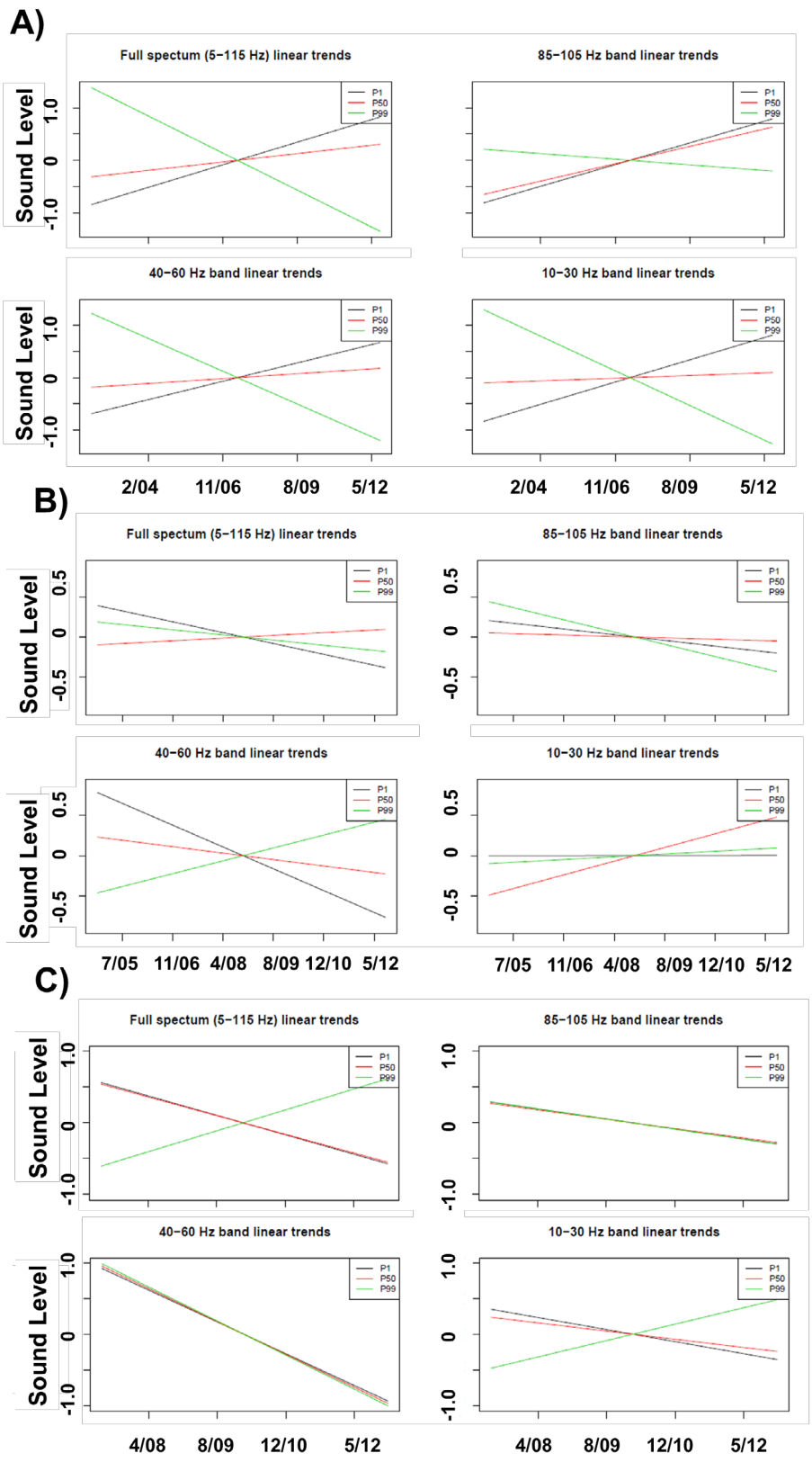

Figure 2. Summary of linear trends for the full spectrum and 20-Hz band analyses from the North sides of A) Diego Garcia (H08 Indian Ocean), B) Ascension Island (H10 S. Atlantic Ocean), and C) Wake Island (H11 Equatorial Pacific Ocean) locations.

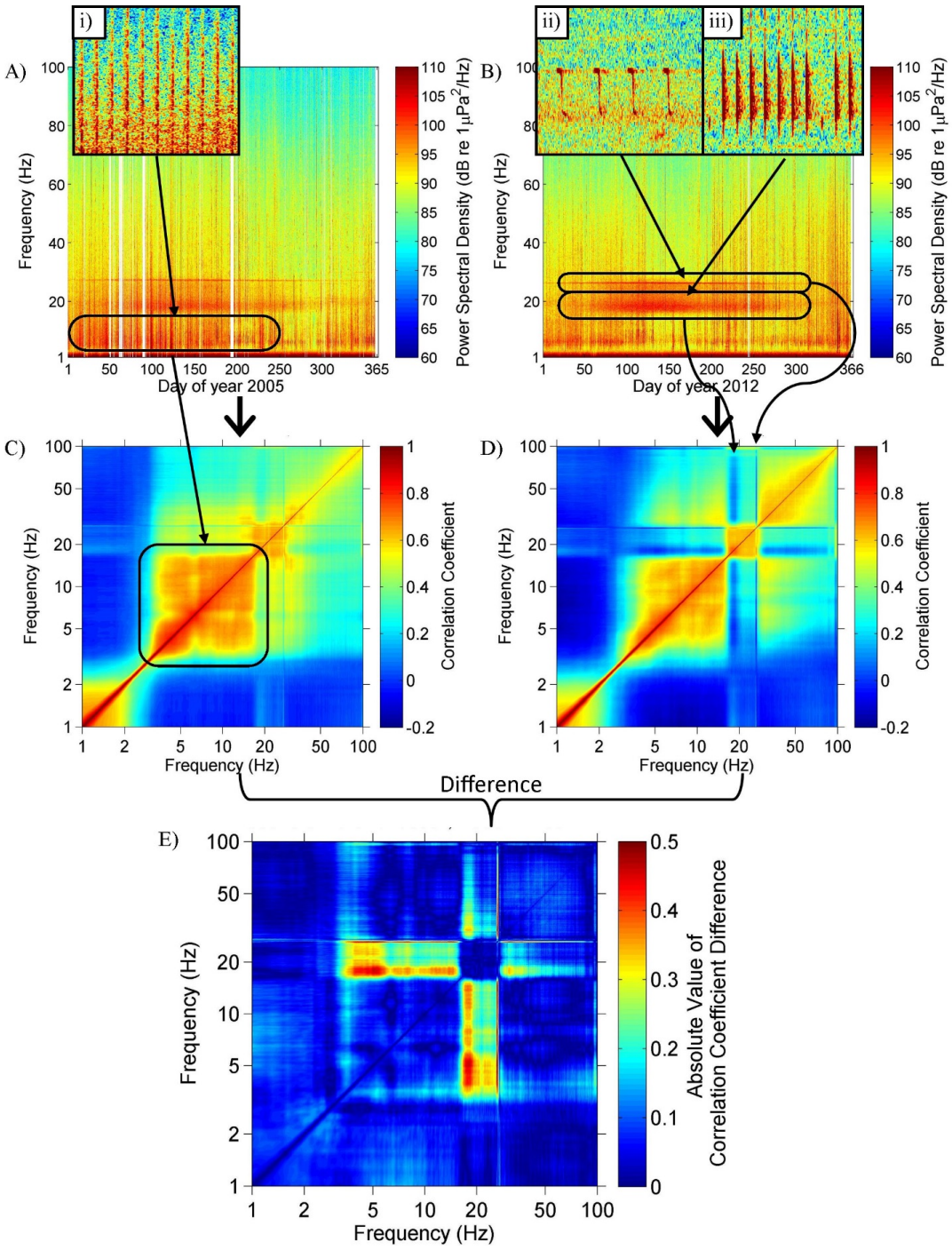

Figure 3. Demonstration of the procedure used to create a frequency correlation difference matrix. Starting with yearly spectrograms from the H10 Ascension Island South (S1) location in 2005 (A) and 2012 (B), the correlation coefficients between spectral levels at different frequencies are computed to form a frequency correlation matrix for the same location in 2005 (C) and 2012 (D). The frequency correlation matrices are then subtracted from each other to find the correlation difference matrix between the two years at the same location. Circles highlight specific features discussed in the text.

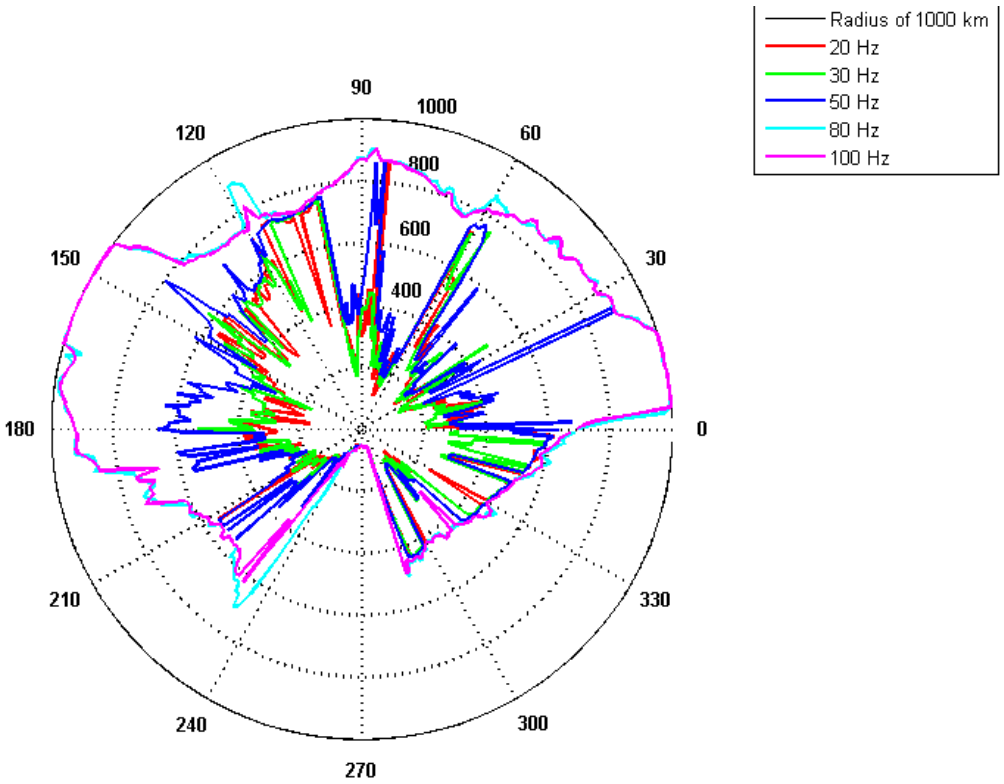

Figure 4. Full 360^{0} signal DA from H08N1 Diego Garcia North in the Indian Ocean for the month of November 2002. The signal detection area was modelled out to 1000 km for the 5 specified frequencies.

A)

Variance decomposition proportions

CondInd	X1	X2	X3	X4	X5	X6	X7
1	-----	-----	-----	-----	-----	-----	-----
10	-----	-----	-----	-----	-----	-----	-----
15	-----	-----	-----	0.715	-----	-----	-----
32	-----	-----	-----	-----	0.874	0.721	-----
110	-----	-----	-----	-----	-----	-----	0.566
153	-----	-----	0.508	-----	-----	-----	-----
336	0.905	0.886	-----	-----	-----	-----	-----
VIF:	3.2	2.6	1.5	1.6	3.8	4.8	2.0

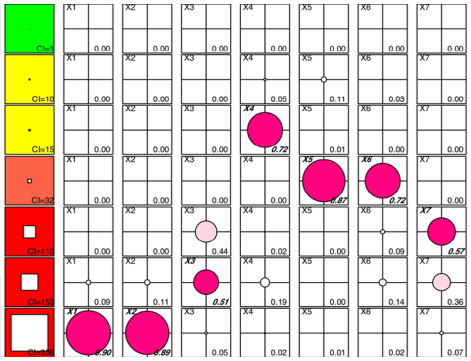

X1=P1Noise
X2=P50Noise
X3=P99Noise
X4=TotalShipping
X5=chl
X6=PP
X7=SST

Variance decomposition proportions

CondInd	X1	X2	X3	X4	X5	X6
1	-----	-----	-----	-----	-----	-----
11	-----	-----	-----	-----	0.564	-----
13	-----	-----	-----	0.742	-----	-----
96	-----	-----	-----	-----	-----	0.773
132	-----	-----	0.675	-----	-----	-----
308	0.906	0.915	-----	-----	-----	-----
VIF:	3.1	2.6	1.5	1.6	1.7	1.6

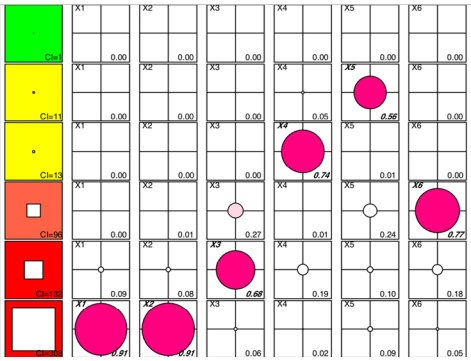

X1=P1Noise
X2=P50Noise
X3=P99Noise
X4=TotalShipping
X5=chl
X6=SST

B)

Variance decomposition proportions

CondInd	X1	X2	X3	X4	X5	X6	X7
1	-----	-----	-----	-----	-----	-----	-----
10	-----	-----	-----	0.669	-----	-----	-----
14	-----	-----	-----	-----	-----	-----	-----
35	-----	-----	-----	-----	-----	-----	-----
85	-----	-----	-----	-----	-----	0.506	0.813
152	-----	-----	0.984	-----	-----	-----	-----
910	0.990	0.992	-----	-----	-----	-----	-----
VIF:	9.4	7.4	1.1	1.2	4.8	6.2	3.1

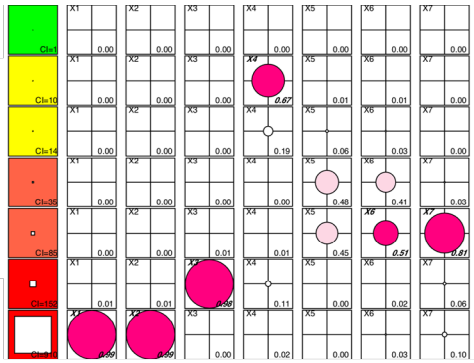

X1=P1
X2=P50
X3=P99
X4=TotalShipping
X5=chl
X6=PP
X7=SST

Variance decomposition proportions

CondInd	X1	X2	X3	X4	X5	X6
1	-----	-----	-----	-----	-----	-----
10	-----	-----	-----	0.799	-----	-----
15	-----	-----	-----	-----	0.802	-----
58	-----	-----	-----	-----	-----	0.893
140	-----	-----	0.978	-----	-----	-----
830	0.990	0.992	-----	-----	-----	-----
VIF:	8.8	7.3	1.1	1.2	1.3	1.8

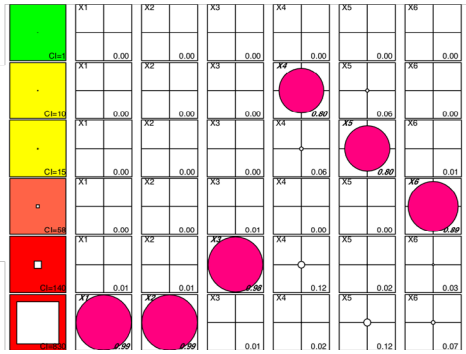

X1=P1
X2=P50
X3=P99
X4=TotalShipping
X5=chl
X6=SST

Figure 5. Colinearity plots for all predictor variables from A) Diego Garcia North H08N1 and B) Wake Island North H11N1. The Top plot show high colinearity between primary production (PP), chlorophyll, and SST. The Bottom plots removed PP and only show colinearaity between P1 and P50 sound levels.

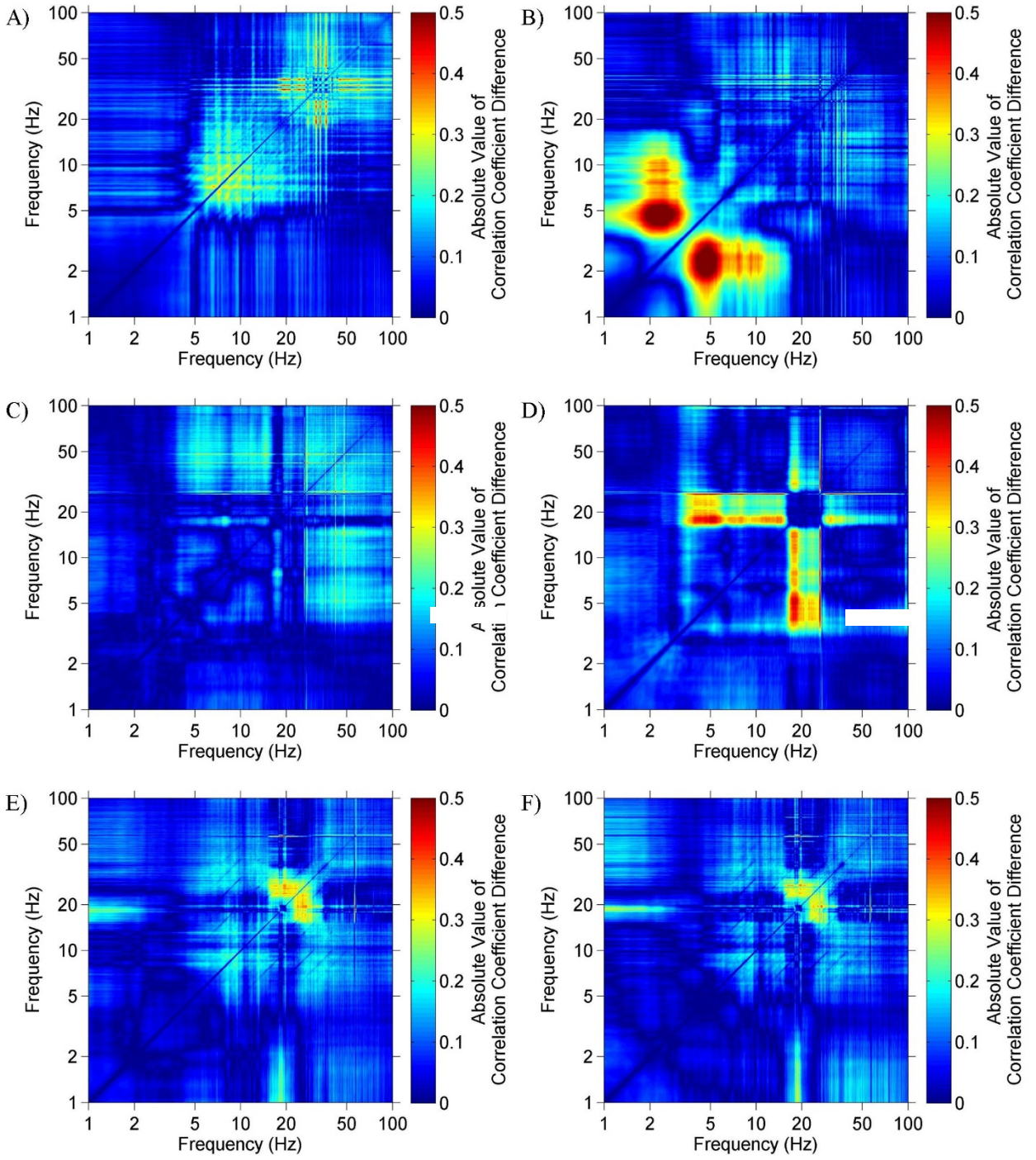

Figure 6. Frequency correlation difference matrices demonstrating the difference in frequency correlation between: 2003 and 2012 for H08 Diego Garcia North (N1) (A) and South (S2) (B), 20005 and 2012 for H10 Ascension Island North (N1) (C) and South (S1) (D), and the period from May 2007 to April 2008 and 2012 for H11 Wake Island North (N1) (E) and South (S1) (F).

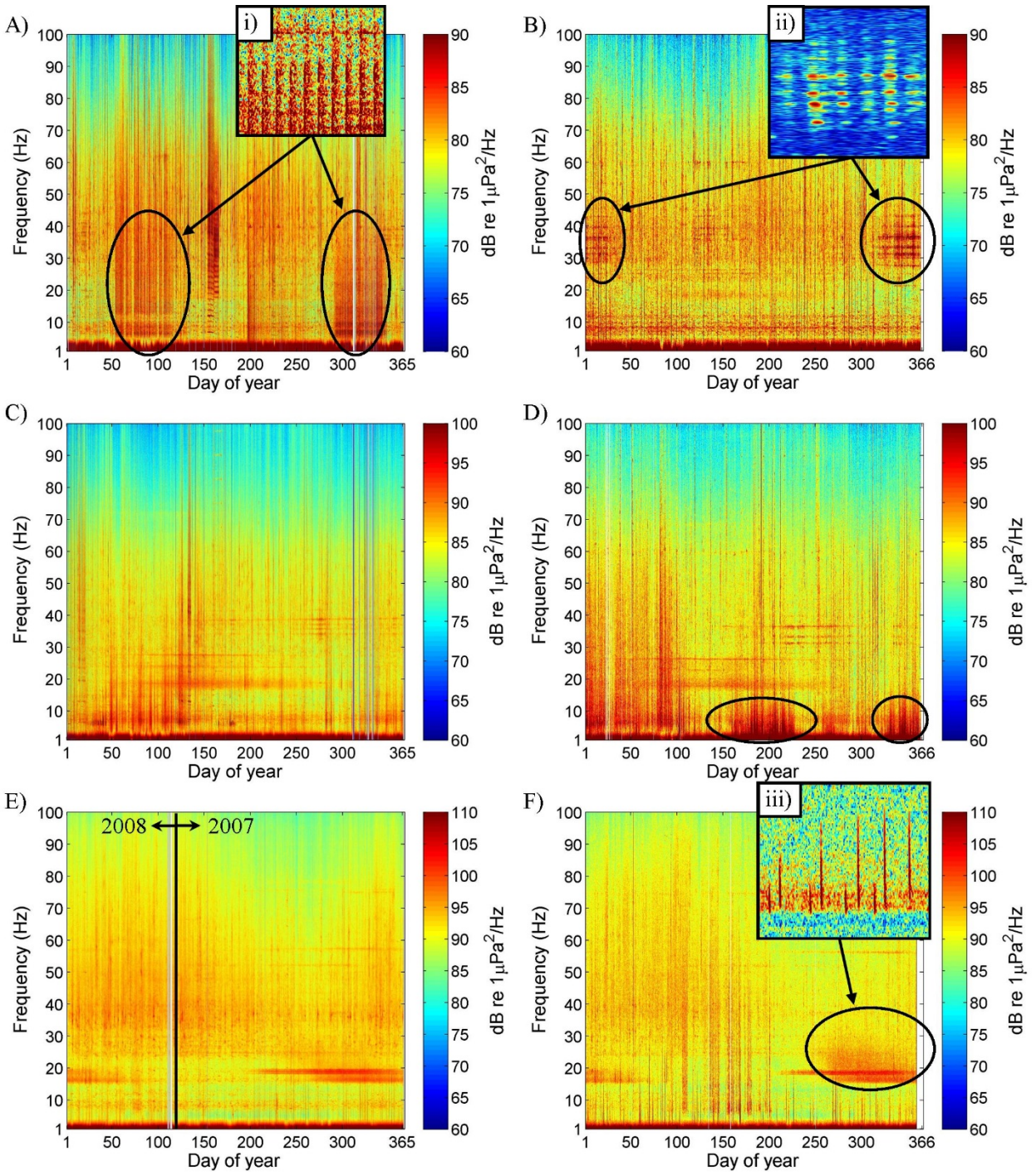

Figure 7. Yearlong spectrograms of the sound field at: Diego Garcia North (N1) in (A) 2003 and (B) 2012, Diego Garcia South (S2) in (C) 2003 and (D) 2012, and Wake Island South (S1) from (E) May 2007 to April 2008 and (F) 2012. Circles highlight specific features discussed in the text.

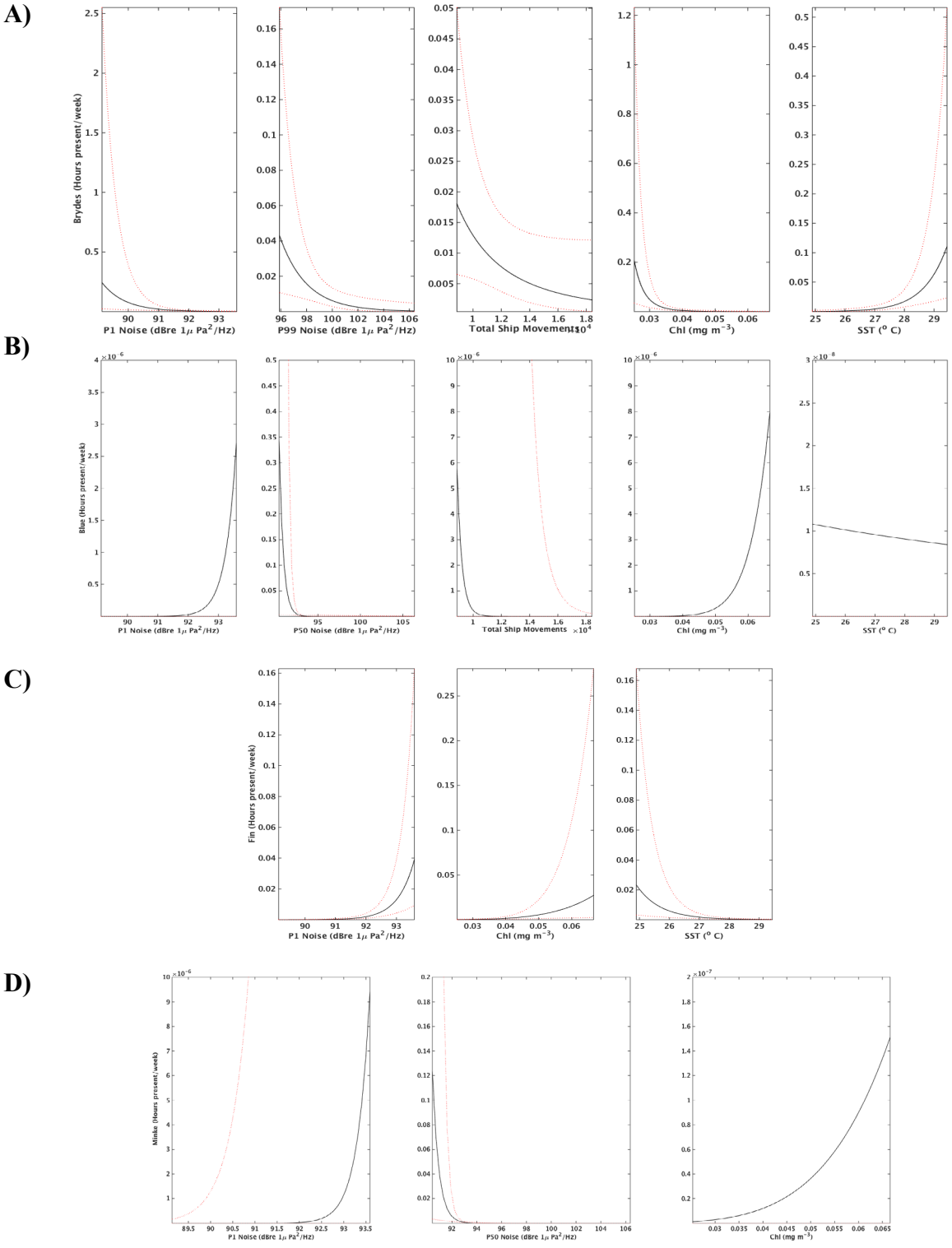

Figure 8. Impact directionality plots for significant predictors of A) Bryde's whale, B) blue whale, C) fin whale, and D) minke whale temporal vocal patterns at Wake Island H11 in the Pacific Ocean. Red lines are 95% confidence intervals.

A)

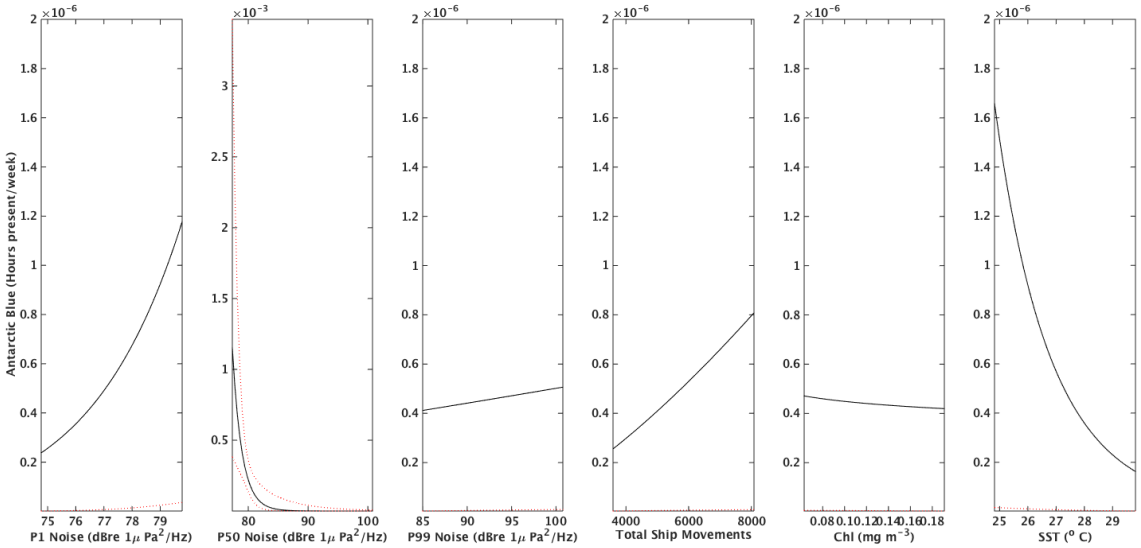
Antarctic Blue (Hours present/week)
P1 Noise (dBre 1μ Pa²/Hz)
P50 Noise (dBre 1μ Pa²/Hz)
P99 Noise (dBre 1μ Pa²/Hz)
Total Ship Movements
Chl (mg m⁻³)
SST (° C)

B)

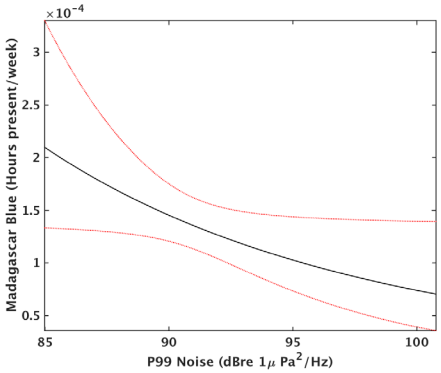
Madagascar Blue (Hours present/week)
P99 Noise (dBre 1μ Pa²/Hz)

C)

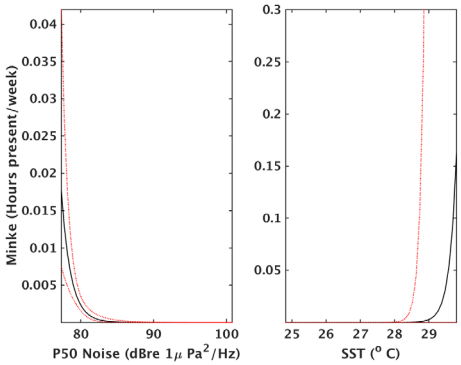
Minke (Hours present/week)
P50 Noise (dBre 1μ Pa²/Hz)
SST (° C)

D)

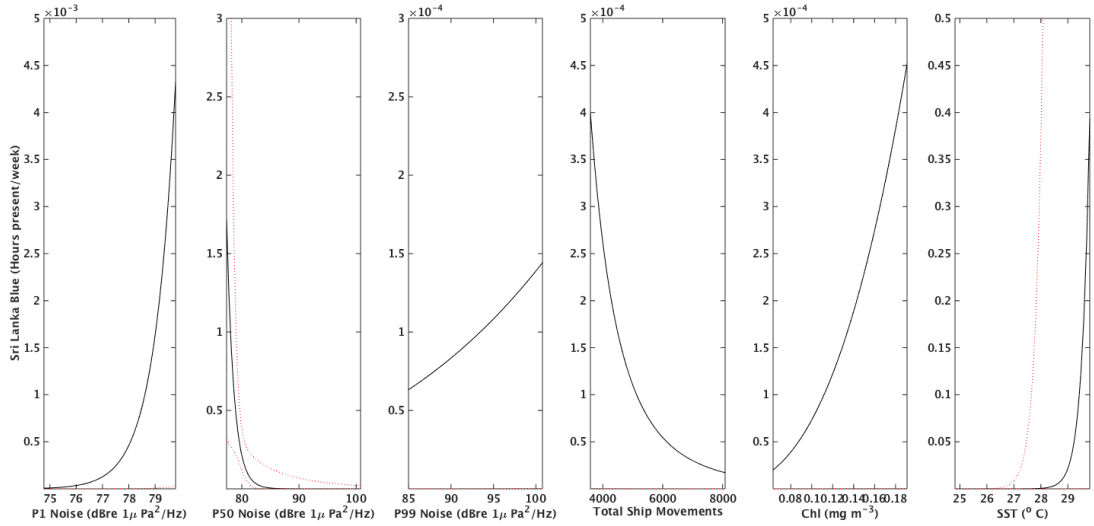
Sri Lanka Blue (Hours present/week)
P1 Noise (dBre 1μ Pa²/Hz)
P50 Noise (dBre 1μ Pa²/Hz)
P99 Noise (dBre 1μ Pa²/Hz)
Total Ship Movements
Chl (mg m⁻³)
SST (° C)

E)

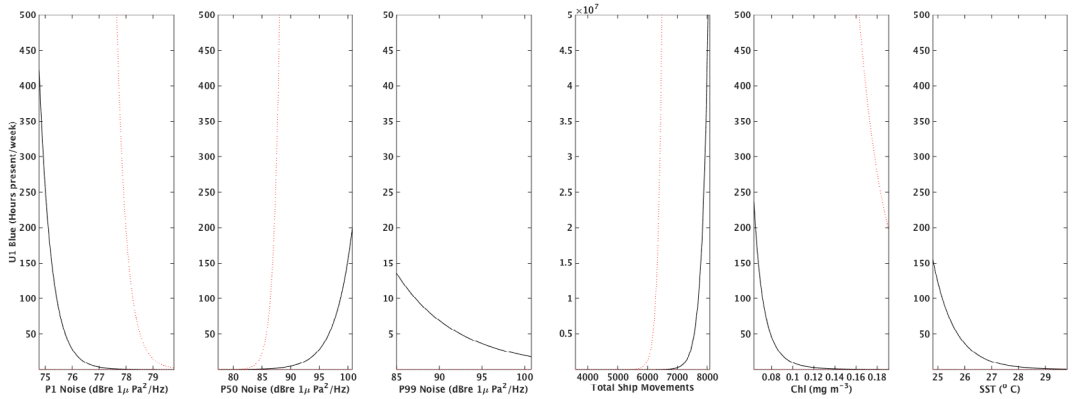

F)

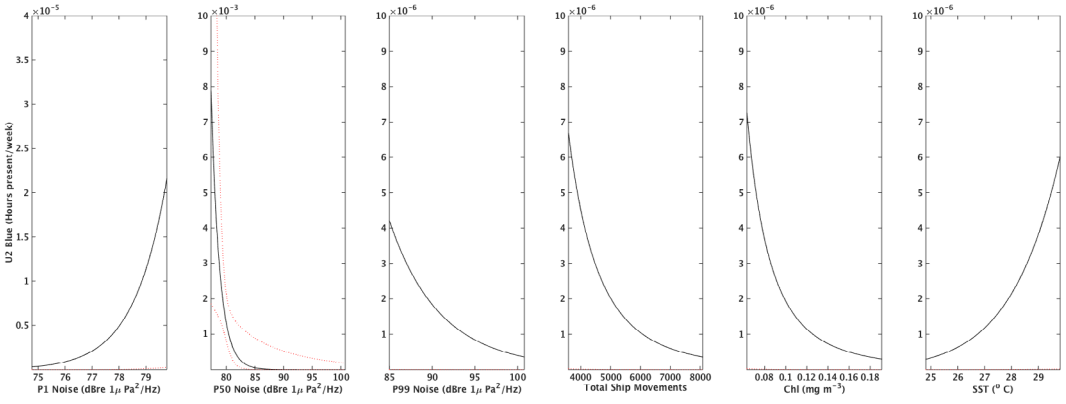

G)

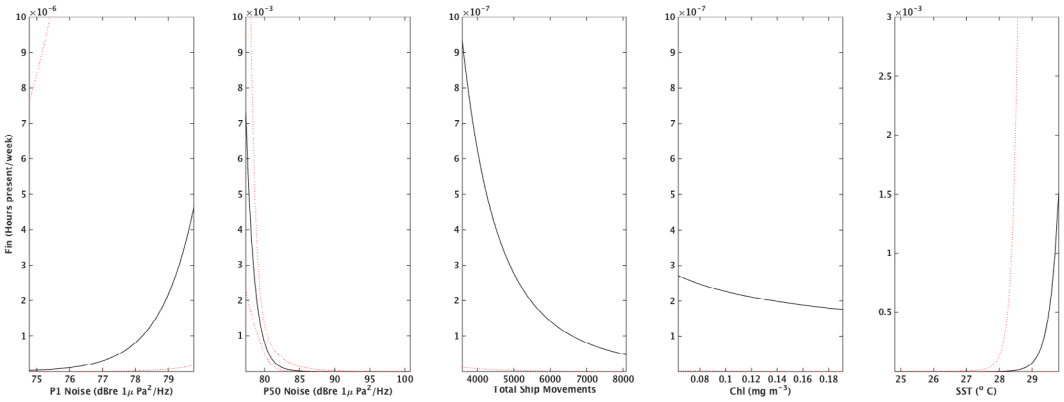

Figure 9. Impact directionality plots for significant predictors of A) Antarctic blue, B) Madagascar blue, C) minke, D) Sri Lankan blue, E) U1 blue call type, F) U2 blue call type, and G) fin whale temporal vocal patterns at Diego Garcia H08 in the Indian Ocean. Red lines are 95% confidence intervals.